Journal of Hydroscience and Hydraulic Engineering
Vol. 19, No.1 May, 2001, 97-105

DEVELOPMENT OF MULTIBLOCK-PARALLEL COMPUTATION METHOD WITH CURVILINEAR COORDINATES AND ITS BASIC FEATURES

By

S. Ushijima and I. Nezu

Department of Global Environment Engineering, Kyoto University
Kyoto-shi, 606-8501, Japan
ushijima@gee.kyoto-u.ac.jp

N. Tanaka and N. Yoneyama

Central Research Institute of Electric Power Industry
1646 Abiko, Abiko-shi, Japan

SYNOPSIS

This paper concerns a multiblock-parallel computation technique for three-dimensional turbulent flows, which is advantageous to deal with complicated boundary shapes and to improve computational efficiency as well. A computational domain is decomposed into multiple sub-blocks and their geometries are represented by curvilinear coordinates. The multiple sub-blocks are connected on their surfaces without overlap, so that the grids near the shared surfaces can be easily generated even when the three-dimensional connected regions have complex geometries. The spatial interpolation for some of the variables are performed with a cubic spline function, which prevents the first-order numerical error arising between sub-blocks. As a result of the parallel computations for laminar flows with a moving wall and pressure gradients, it was confirmed that the computational speed is about twice when using four workstations with 130,000 computational nodes.

INTRODUCTION

In the present study, a new computational technique is developed for three-dimensional turbulent flows confined in the complicated-shaped boundaries as found in actual hydraulics structures. This technique is based on the domain decomposition method in which a computational volume is separated into multiple sub-blocks and their boundary shapes are represented with boundary-fitted coordinates. While the boundary-fitted coordinate system is one of the most effective methods which allow us to deal with the arbitrarily-shaped boundaries (1), it is sometimes impossible to generate coordinates against extremely complicated objects, such as the pipe systems with branch and combination, due to the difficulty of grid-point mapping. For such problems, the domain decomposition method, employed in our computational method, is much advantageous and it can be applied to the computational domain including discontinuity regions.

In addition, since the structured grid system is adopted in the present method, it is relatively easy to increase the accuracy related to the discretization and to introduce higher-order turbulence models rather than the other computational methods, such as finite element methods and finite volume methods based on unstructured grid systems, which are also applicable to the complicated geometries.

Among the domain decomposition methods, the multigrid systems with overlap (2) and without overlap (3) have been proposed in the past. While the methods with overlap have the reasonable accuracy (4), it is difficult to generate the three-dimensional grid points in the complicated geometries. For this reason, a non-overlap method is employed in the present study and some of the variables on

the boundaries shared by two sub-blocks are spatially interpolated with the cubic spline function to increase the accuracy. The validity of this method is demonstrated in the computation of the laminar flows confined in the parallel plates.

The computations of the flows in the sub-blocks are simultaneously performed with a cluster of multiple workstations connected with network. As a result of this parallel computations for laminar flows with a moving wall and pressure gradients, it is confirmed that the computational speed is about twice using four workstations with 130,000 computational nodes.

NUMERICAL PROCEDURE

Domain Decomposition and Grid Generation

The three-dimensional computational domain is decomposed into multiple sub-blocks with the sections arbitrarily set up by a user. In the setting up of the multiple sub-blocks, it may be desirable to take account of the balance of the grid numbers in sub-blocks in order to improve the computational efficiency in the parallel computation. Figure 1 shows the schematic view of the block decomposition.

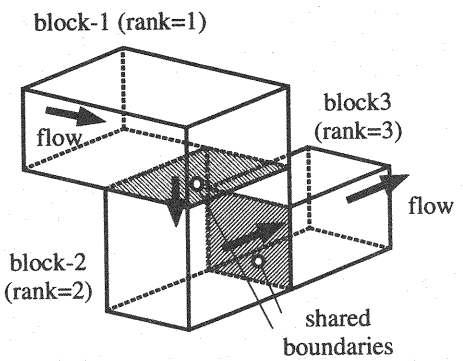

Fig. 1 Schematic view of the block decomposition

The sequential numbers (rank numbers) are given to the generated sub-blocks, as shown in Fig.1 and the boundary surfaces shared by two sub-blocks are specified by taking account of the connection of sub-blocks.

This block decomposition allows us to generate boundary-fitted coordinates for the sub-blocks which have largely simplified geometries compared with the whole computational domain before decomposition. This curvilinear coordinate system is generated with the following equation which is transformed from the Poisson equations for coordinates, as done by Thompson (1):

$$\left(\frac{\partial^2 x_i}{\partial\xi_p\partial\xi_q}\right)^*\left(\frac{\partial\xi_p}{\partial x_j}\right)^*\left(\frac{\partial\xi_q}{\partial x_j}\right)^* + \frac{\partial^2 x_i}{\partial\xi_r\partial\xi_s}\left(\frac{\partial\xi_r}{\partial x_j}\right)^*\left(\frac{\partial\xi_s}{\partial x_j}\right)^* + P_m\left(\frac{\partial x_i}{\partial\xi_m}\right)^* = 0 \qquad (1)$$

Here x_i and ξ_m are coordinates in the physical and transformed spaces, respectively. The terms having asterisks (*) are evaluated with the cubic spline function, rather than central differencing, to increase the numerical accuracy. The control function, given by P_m in Eq.1, is used to adjust the mesh intervals in the physical space.

The unit computational volume consists of 27 grid points in the transformed space. While the staggered grid arrangement is employed for the contravariant velocity components and pressure variables, the intervals of the grid points are adjusted near the boundary regions so that the variables are placed on the boundary surfaces. This procedure means that no variables are defined outside of the computational domain and it allows us to reasonably set up Dirichlet and Neumann boundary conditions, especially in the vicinity of the surface shared by sub-blocks. Figure 2 shows the example of this grid-point arrangement on a two-dimensional plane near the corner.

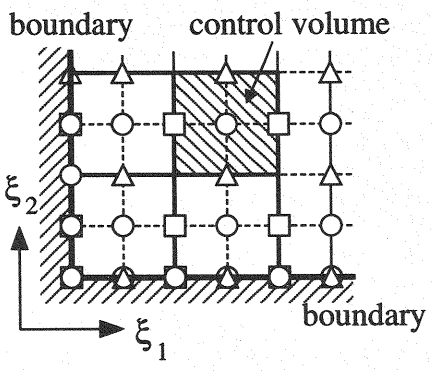

Fig. 2 Grid-point arrangement near the corner on a 2D plane ($\bigcirc = p$, $\square = U_1$, $\triangle = U_2$)

Computation of Fluid in a Sub-Block

In the generated sub-blocks, the transformed governing equations for turbulent flows are discretized with a finite difference method. The equations with a two-equation turbulence model are given as follows:

(1) momentum equation

$$\frac{Du_i}{Dt} = -\frac{1}{\rho}\frac{\partial p}{\partial \xi_m}\frac{\partial \xi_m}{\partial x_i} + F_i + (\nu + \epsilon_M)\left(\frac{\partial^2 u_i}{\partial \xi_m \partial \xi_n}\frac{\partial \xi_m}{\partial x_j}\frac{\partial \xi_n}{\partial x_j} + P_m \frac{\partial u_i}{\partial \xi_m}\right) + \frac{\partial \epsilon_M}{\partial \xi_m}\frac{\partial \xi_m}{\partial x_j}\left(\frac{\partial u_i}{\partial \xi_n}\frac{\partial \xi_n}{\partial x_j}\frac{\partial u_j}{\partial \xi_n}\frac{\partial \xi_n}{\partial x_i}\right) - \frac{3}{2}\frac{\partial k}{\partial \xi_m}\frac{\partial \xi_m}{\partial x_i} \tag{2}$$

(2) transport equation for turbulence energy k

$$\frac{Dk}{Dt} = \epsilon_M\left(\frac{\partial u_i}{\partial \xi_n}\frac{\partial \xi_n}{\partial x_j} + \frac{\partial u_j}{\partial \xi_n}\frac{\partial \xi_n}{\partial x_i}\right)\frac{\partial u_i}{\partial \xi_m}\frac{\partial \xi_m}{\partial x_j} + \left(\nu + \frac{C_k}{C_\nu}\epsilon_M\right)\left(\frac{\partial^2 k}{\partial \xi_m \partial \xi_n}\frac{\partial \xi_m}{\partial x_j}\frac{\partial \xi_n}{\partial x_j} + P_m \frac{\partial k}{\partial \xi_m}\right) + \frac{C_k}{C_\nu}\frac{\partial \epsilon_M}{\partial \xi_m}\frac{\partial \xi_m}{\partial x_j}\frac{\partial k}{\partial \xi_n}\frac{\partial \xi_n}{\partial x_j} - \epsilon \tag{3}$$

(3) transport equation for the dissipation rate of k

$$\frac{D\epsilon}{Dt} = C_{\epsilon 1}\frac{\epsilon}{k}\epsilon_M\left(\frac{\partial u_i}{\partial \xi_n}\frac{\partial \xi_n}{\partial x_j} + \frac{\partial u_j}{\partial \xi_n}\frac{\partial \xi_n}{\partial x_i}\right)\frac{\partial u_i}{\partial \xi_m}\frac{\partial \xi_m}{\partial x_j} + \left(\nu + \frac{C_\epsilon}{C_\nu}\epsilon_M\right)\left(\frac{\partial^2 \epsilon}{\partial \xi_m \partial \xi_n}\frac{\partial \xi_m}{\partial x_j}\frac{\partial \xi_n}{\partial x_j} + P_m \frac{\partial \epsilon}{\partial \xi_m}\right) + \frac{C_\epsilon}{C_\nu}\frac{\partial \epsilon_M}{\partial \xi_m}\frac{\partial \xi_m}{\partial x_j}\frac{\partial \epsilon}{\partial \xi_n}\frac{\partial \xi_n}{\partial x_j} - C_{\epsilon 2}\frac{\epsilon^2}{k} \tag{4}$$

Here u_i and F_i are average velocity component and external force in x_i direction, respectively, and p is pressure, ρ density of fluid, ν kinematic viscosity and ϵ_M eddy viscosity. The model constants, C_k, C_ν, C_ϵ, $C_{\epsilon 1}$ and $C_{\epsilon 2}$, are given as indicated by Rodi (5). The Lagrangian differential operator, appearing on the left hand side of the above governing equations, is given by

$$\frac{D}{Dt} = \frac{\partial}{\partial \tau} + U_m \frac{\partial}{\partial \xi_m} \tag{5}$$

where U_m is the contravariant velocity component and t and τ are time variables in physical and transformed spaces, respectively, which are identical in the present paper.

The governing equations are discretized in a Lagrangian scheme in the transformed space. The momentum equation given by Eq.2, for example, is written in the following form (6):

$$u_i^{n+1} = u_i'^n + \left[-PG_i^{n+1} + F_i^n + \left(\frac{3}{2}D_i'^n - \frac{1}{2}D''^{n-1}_i\right)\right]\Delta t \tag{6}$$

where PG_i and D_i are pressure-gradient and diffusion terms included in the momentum equation. The signs, prime and double prime, in Eq.6 indicate the variables located at the upstream positions at $n-1$ and $n-2$ time steps, respectively. The other governing equations are discretized in the similar way to the momentum equation.

The convection term, corresponding to the first term on the right hand side of Eq.6, is calculated with the LCSI method proposed by Ushijima (6). As a result, this term is evaluated with the third-order accuracy by using the surrounding 64 variables in the three-dimensional space, which allows us to have more accurate results than the third-order upwind differencing method.

The pressure field is calculated with the following equation which is derived from the continuity and momentum equations:

$$\frac{\partial^2 p^{n+1}}{\partial\xi_m \partial\xi_n}\left(\frac{\partial\xi_m}{\partial x_j}\right)\left(\frac{\partial\xi_n}{\partial x_j}\right) + P_m \frac{\partial p^{n+1}}{\partial\xi_m} = \frac{\rho}{\Delta t}\left(\frac{\partial U'^n_m}{\partial\xi_m} + \frac{\partial FU_i}{\partial\xi_m}\frac{\partial\xi_m}{\partial x_i}\Delta t\right) \equiv RHS \tag{7}$$

While the grid positions for pressure variables are changed near the boundaries, as shown in Fig.2, the second-order accuracy is preserved by using more number of variables than in the internal area. Thus, the maximum number of the surrounding pressure variables, p_{pqr}, used in the computation of p_{ijk} is 21 in the vicinity of the boundary area, as indicated in the following algebraic equation:

$$c_0 p^{n+1}_{ijk} + \sum_{m=1}^{21} c_m p^{n+1}_{pqr} = RHS_{ijk} \tag{8}$$

where c_0 and c_m are the coefficients including the derivatives of coordinates.

Since these treatments for the governing equations are common in all sub-blocks, the source program related to these procedures are gathered in a common directory. On the other hand, the information inherent to the sub-blocks, such as the geometry, boundary conditions and connection with other sub-blocks, is put in the local directories of corresponding sub-blocks. In the compiling of the source files, the necessary files in the common directory and in the local directories are selected and then they are converted to the executable form.

Message Passing in Parallel Computation

The parallel computations for grid generation and for the governing equations of fluid flows in the sub-blocks are simultaneously performed in multiple workstations (COMPAQ Alpha21164 500MHz) connected with a network system. The software libraries related to the message passings and other procedures in parallel computation are provided by LAM (http://www.mpi.nd.edu/lam/), which is based on the standard MPI (Message Passing Interface) instructions (7). Since LAM allows us to perform parallel computation on general workstations connected with networks, no special parallel computers are required for the present numerical method.

In the multiblock system, it is necessary for the sub-blocks sharing common boundaries to exchange their calculated variables at the suitable computational steps. To perform this multiblock communication efficiently, a master-slave model is adopted as shown in Fig.3. The slave processes are assigned to sub-blocks one by one and they conduct the grid generations and fluid computations in the appointed sub-blocks. The calculated results located near the shared boundaries are gathered to the master process. The master process, which has received computed results from multiple sub-blocks, performs spatial interpolation and other numerical procedures and then sends them back to the sub-blocks. Consequently, the multiblock communication is largely simplified by employing this master-slave type model.

In the computations, as shown in Fig.3, firstly the generated coordinates are transferred to the master process. Then the computations of turbulent flows start with the given initial conditions. In the iterative calculation of the pressure field, the variables are communicated among the slave processes through the master process at every appointed iterative step-number. This data communication allows us to obtain the adequately converged the pressure fields in the whole computational domain. When

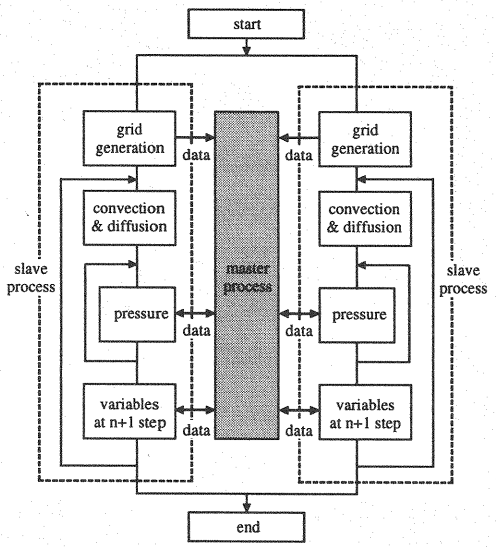

Fig. 3 Flowchart of multiblock-parallel computation

all variables are calculated at the new $(n+1)$ computational step, they are transferred to the master process and some of them are spatially interpolated. This numerical procedures in the master process are necessary particularly when the computational grids are not coincident with each other on the shared boundary. The results of the master process are returned to the slave processes and the computations at the following time step proceed independently in multiple sub-blocks.

Spatial Interpolation between Blocks

The variables located on the shared boundary are used as boundary conditions in the sub-block fluid computations. On this common boundary, scalar variables except pressure and the velocity components parallel to the boundary face are interpolated with the variables included in two sub-blocks. In order to increase the numerical accuracy in this inter-block evaluation, the cubic spline function is employed in the present study. As indicated in Fig.4, when block-A and block-B are connected and the variable on the common boundary is given by ϕ_0 and those included inside of the sub-blocks are given by ϕ_{Ai} and ϕ_{Bi} $(i = 1, 2, ...)$, ϕ_0 is evaluated with the following relationship:

$$\phi_0 = M_{A1}\frac{d_{B1}^3}{6d} + M_{B1}\frac{d_{A1}^3}{6d} + \left(\phi_{A1} - \frac{M_{A1}d^2}{6}\right)\frac{d_{B1}}{d} + \left(\phi_{B1} - \frac{M_{B1}d^2}{6}\right)\frac{d_{A1}}{d} \tag{9}$$

where M_{A1} and M_{B1} are second derivatives of ϕ and they are calculated from two third-order polynomial functions, which are uniquely determined with the four variables ϕ_{Ai} and ϕ_{Bi} $(i = 1, 2, ..., 4)$. In Eq.9, d, d_{A1} and d_{B1} are the distance between ϕ_{A1} and ϕ_{B1}, between ϕ_0 and ϕ_{A1} or ϕ_{B1}, respectively.

In the actual computation, the second derivatives M_{A1} and M_{B1} are calculated in the slave processes and they are transferred to the master process. In the master process, the variables on the common boundary are interpolated with Eq.(9) and then the results are returned to the slave processes.

NUMERICAL ACCURACY AND COMPUTATIONAL EFFICIENCY

Inter-block Spatial Interpolation

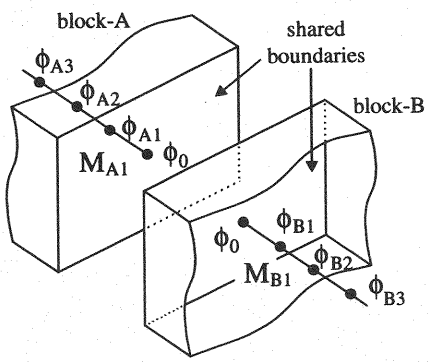

Fig. 4 interblock evaluation on the common boundary

The present computational scheme and other numerical procedures have been applied to the various flows, such as the three-dimensional flows in a curved pipe and thermally stratified flows in a curved duct (6), and its validity has been demonstrated. The computational accuracy, however, is not certain with the multiblock system especially near the boundaries shared by sub-blocks. Thus, the present numerical technique is applied to the laminar flow confined in two parallel walls, whose velocity profiles are theoretically known.

Figure 5 shows the computational domain and boundary conditions about this problem. The domain is a cubic volume with unit length in each direction.

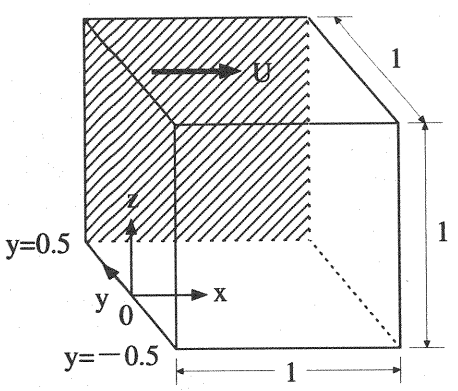

Fig. 5 Computational domain

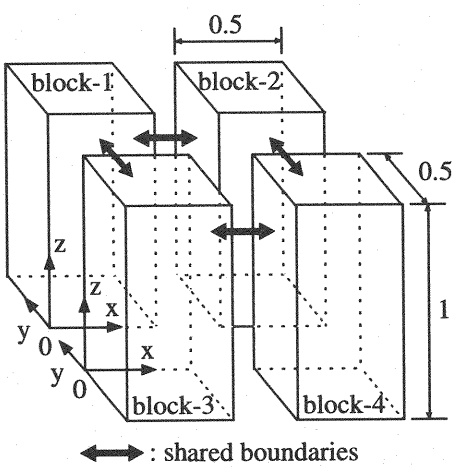

Fig. 6 Domain decomposition

The boundary plane at $y = 0.5$ is a movable wall with the speed U in x direction and the other surface at $y = -0.5$ is a fixed wall. Two surfaces vertical to the z axis are free-slip boundaries. While the cyclic boundary conditions for velocity are applied to the upstream boundary at $x = 0$ and the downstream one at $x = 1$, the constant pressure difference is also put on these two boundaries. The fluid in the computational domain starts to flow due to the movement of the wall and pressure gradient dp/dx in x direction. The velocity field is finally in the steady state after sufficient time.

In this condition, the theoretical velocity profile is given by

$$u(y) = U(0.5 + y) - \frac{1}{2\mu}\frac{dp}{dx}(0.25 - y^2) \tag{10}$$

When the pressure gradient equals zero, it becomes the Couette flow with the following linear velocity profile:

$$u(y) = U(0.5 + y) \tag{11}$$

From Eq.(10), the following non-dimensional pressure gradient P is defined:

$$P = -\frac{1}{2\mu}\frac{dp}{dx}\frac{1}{U} \tag{12}$$

In the multiblock computations, the domain was decomposed into four sub-blocks, as shown in Fig.5 (a), and both linear and spline interpolations were employed as the inter-block evaluations and two results were compared. All intervals of grid points are constant and a control function P_m in Eq.(1) was set at zero. The unsteady calculations were performed from the initial static velocity field until the velocity profiles are almost in steady state with 10,000 computational steps.

Figures 7 (a) and (b) show the comparisons between theoretical and computational results. As shown in Fig.7, the discrepancies between the theory and the computational results with the inter-block linear interpolation become large with the increase of P. In particular, as indicated in Fig.7 (b), the maximum velocity is evaluated smaller than the theory when $U = 0$ and $P = 5$. In contrast, the computational results with inter-block spline interpolation agree well with the theoretical results.

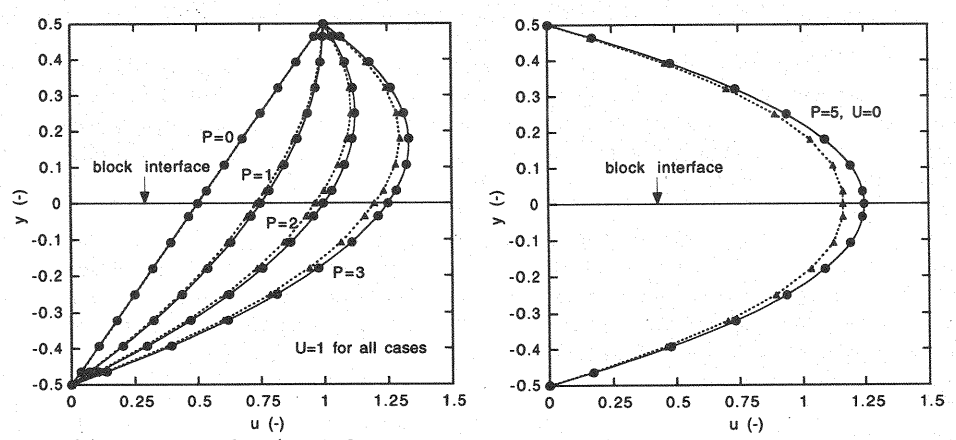

(a) velocity profiles (— = theory, ▲ and broken lines = linear interpolation, ● = spline interpolation)

(b) velocity profiles (symbols are same as left)

Fig. 7 Comparison of velocity profiles between linear and spline interpolations

Improvement of Computational Efficiency

The computational efficiency was compared between single-block and multiblock computations with four workstations. The results are shown in Fig.8, which indicates the computational time against the mesh number.

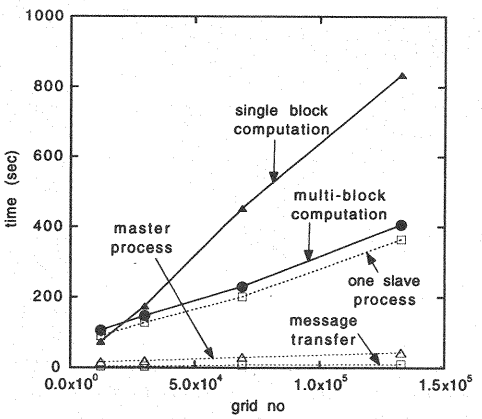

Fig. 8 Comparison of computational efficiency

Although the multiblock computation is not advantageous in terms of the computational time when mesh number is less than 20,000, as shown in Fig.8, its computational efficiency is obviously improved when lager number of grid points are used. As a result, the computational speed reaches about twice compared with the single-block condition when the mesh number is about 130,000.

CONCLUDING REMARKS

In the present study, a multiblock-parallel computation technique has been developed for three-dimensional turbulent flows, which allows us to deal with the complicated boundary shapes and to improve computational efficiency as well. In this computational method, a computational domain is decomposed into multiple sub-blocks and their geometries are represented by curvilinear coordinates. The governing equations for turbulent flows are discretized in a Lagrangian scheme. The multiple sub-blocks are connected on their surfaces without overlap, so that the grids near the shared surfaces can be easily generated even when the three-dimensional connected regions have complex geometries. The spatial interpolation for some of the variables are performed with the cubic spline function, which prevents the first-order numerical error arising between sub-blocks. As a result of the parallel computations for laminar flows with a moving wall and pressure gradients, it was confirmed that the computational speed is about twice when we use four workstations with 130,000 computational nodes.

REFERENCES

1. Thompson, J. F., Warsi, Z. U. A., and Mastin, C. W. : Numerical Grid Generatio, Elsevier, New York, 1985.

2. Shyy, W., Wright, J., and Liu, J. : A multilevel composite grid method for fluid flow computations, AIAA-93-0768, 1993.

3. Perng C. Y. and Street R. L. : A coupled multi-grid domain splitting technique for simulating incompressible flows in geometrically complex domain, Int. J. Numer. Meth. Fluids, 13, pp.269 286, 1991.

4. Shyy, W., Liu, J., and Wright, J. : Pressure based viscous flow computation using multiblock overlapped curvilinear grids, Numerical Heat Transfer, Part B, vol.25, pp.39 59, 1994.

5. Rodi, W. : Turbulence models, their application in hydraulics, A state of the art review presented by the IAHR section on fundamentals of division II experimental, and mathematical fluid dynamics, 1980.

6. Ushijima, S. : Prediction of thermal stratification in a curved duct with 3D boundary-fitted coordinates, International Journal for Numerical Methods in Fluids, Vol.19, pp.647-665, 1994.

7. Gropp, W., Lusk, E., and Skjellum, A. : Using MPI, The MIT Press, 1994.

APPENDIX-NOTATION

The following symbols are used in this paper:

$C_k, C_\nu, C_\epsilon, C_{\epsilon 1}, C_{\epsilon 2}$	= coefficients of turbulence model;
c_0, c_m	= coefficients of pressure Poisson equation;
D/Dt	= Lagrange differential operator;
D_i	= diffusion term in momentum equation;
d	= distance between ϕ_{A1} and ϕ_{B1};
d_{A1}	= distance between ϕ_0 and ϕ_{A1};
d_{B1}	= distance between ϕ_0 and ϕ_{B1};
$doubleprime('')$	= variable at upstream position at n-2 step;
F_i	= external force in x_i direction;
FU_i	= discretized form of right hand side of momentum equation;
k	= turbulence energy;
M_{A1}, M_{B1}	= second derivatives of ϕ near shared boundary;
P	= non-dimensional pressure gradient;
P_m	= contral function;
PG_i	= pressure gradient term in momentum equation;
p	= mean pressure;
$prime(')$	= variable at upstream position at n-1 step;
t	= time in physical space;
U	= wall speed;
U_m	= contravariant velocity component;
u_i	= mean velocity component in x_i direction;
x_i	= coordinates in physical space;
Δt	= time increment;
ϵ	= dissipation rate of turbulence energy;
ϵ_M	= eddy viscosity;
μ	= coefficient of viscosity;
ν	= kinematic viscosity;
ξ_m	= coordinates in transformed space;
ρ	= fluid density;
τ	= time in transformed space;
ϕ_0	= variable on shared boundary;
$\phi_{Ai}, \phi_{Bi} \quad (i = 1, 2, ...)$	= variable near shared boundary;

(Received August 22, 2000 ; revised December 22, 2000)